DISTINCTIVE PATTERNS OF DOMINANT FREQUENCY TRAJECTORY BEHAVIOUR IN DRUG-REFRACTORY PERSISTENT ATRIAL FIBRILLATION: PRELIMINARY CHARACTERISATION OF SPATIO-TEMPORAL INSTABILITY

João Loures Salinet MSc*; Jiun Haur Tuan MD*; Alastair James Sandilands MBBS, PhD; Peter James Stafford MD; Fernando Soares Schlindwein PhD, DSc; Ghulam André Ng MBChB, PhD

*joint first authors

Departments of Engineering and Cardiovascular Sciences, University of Leicester, UK (JLS, FSS, GAN); National Institute for Health Research Leicester Cardiovascular Biomedical Research Unit, Glenfield Hospital, UK (FSS, GAN); University Hospitals of Leicester NHS Trust, UK (JHT, AJS, PJS, GAN)

Correspondence Address:

Professor G. André Ng,
Department of Cardiovascular Sciences,
University of Leicester,
Glenfield General Hospital,
Leicester LE3 9QP
Tel: +44 (0)116 250 2438
Fax: +44 (0)116 287 5792
Email: gan1@le.ac.uk

Running title: Frequency Trajectory of Atrial Fibrillation

Conflict of Interest

GAN has consultancy agreement and has received fellowship support and speakers' honorarium from St. Jude Medical. AJS and PJS have consultancy agreement and have received speakers' honorarium from St. Jude Medical.

Funding Sources

JLS is supported by CNPq-Brazil, process no. 200598/2009-0. FSS gratefully acknowledges financial support from the IPEM, Santander and University of Leicester, UK and GAN acknowledges research grant support from St. Jude Medical, Inc.

Abstract

Introduction: The role of substrates in the maintenance of persistent atrial fibrillation (persAF) remains poorly understood. The use of dominant frequency (DF) mapping to guide catheter ablation has been proposed as a potential strategy, but the characteristics of high DF sites have not been extensively studied. This study aimed to assess the DF spatiotemporal stability using high density non-contact mapping (NCM) in persAF.

Methods and Results: 8 persAF patients were studied using NCM during AF. Ventricular far-field cancellation was performed followed by the calculation of DF using Fast Fourier Transform. Analysis of DF stability and spatiotemporal behaviour were investigated including characteristics of the highest DF areas (HDFAs). A total of 16384 virtual electrograms (VEGMs) and 232 sequential high density 3-dimensional DF maps were analysed. The percentage of DF stable points decreased rapidly over time. Repetition or reappearance of DF values were noted in some instances, occurring within 10 s in most cases. Tracking the HDFAs centre of gravity revealed 3 types of propagation behaviour, namely i) local, ii) cyclical and iii) chaotic activity, with the former 2 patterns accounting for most of the observed events.

Conclusions: DF of individual VEGMs was temporally unstable, although reappearance of DF values occurred at times. Hence targeting sites of 'peak DF' from a single time frame is unlikely to be a reliable ablation strategy. There appears to be a predominance of local and cyclical activity of HDFAs hinting a potentially non-random temporally periodic behaviour which provides further mechanistic insights into the maintenance of persAF.

Key Words: atrial fibrillation, dominant frequency, spectrum analysis, non-contact mapping, dynamics, conduction.

Introduction

Ablation outcomes in persistent atrial fibrillation (persAF) and long-standing persAF remain inferior to that of paroxysmal AF[1, 2], due to a lack of mechanistic insight as to how relevant substrate interacts with triggers and modulating factors to maintain AF. Spectral analysis has been used for the analysis of AF electrograms (EGMs) to identify areas within the atria that contain high dominant frequency (DF) signals which may be responsible for driving the rhythm.[3] It has been suggested that ablation at these sites could be an effective way to terminate AF.[4] In addition, ablation strategies which include pulmonary vein (PV) isolation and additional linear lesions have also been shown to reduce local and/or global DF with an associated beneficial post-ablation outcome, highlighting DF as an important parameter.[5-7] However, DF mapping during AF has been performed largely using point-by-point sequential mapping. Recent reports using non-contact mapping (NCM) in the left atrium (LA) have suggested that DF may not be spatiotemporally stable.[8] In addition, simultaneous bi-atrial contact mapping (CM)[9,10] has also revealed certain characteristic rotor-like behaviours apparently important for ablation. The aim of this study was to characterise the spatiotemporal behaviour of DF during AF using NCM in patients with persAF to help further the understanding of the significance and utility of DF mapping.

Methods

Study population

Patients undergoing catheter ablation of persAF for the first time and with no previous history of heart diseases were recruited (see Table 1 for patients' characteristics). In keeping with the definition of persAF[11], all patients were in AF at the start of the procedure. Approval was obtained from the Local Ethics Committee for patients undergoing AF ablation

including blood sampling and collection of electrical data and all procedures were carried out after informed consent. All antiarrhythmic drugs, apart from amiodarone, were stopped for at least five half-lives before the procedure.

Electrophysiological Study

Once bilateral femoral venous access had been achieved, a deflectable decapolar catheter and a quadripolar catheter were positioned in the coronary sinus and His position, respectively, under fluoroscopic guidance. A single transseptal puncture technique was utilised in all cases to gain access to the LA with the use of a steerable transseptal sheath (Channel, Bard Electrophysiology, USA). A non-contact multi-electrode array (MEA) catheter (EnSite 3000, St Jude Medical, USA) and a conventional deflectable mapping catheter were deployed via transseptal access, into the LA. Patients were anticoagulated with heparin and activated clotting time was maintained at >300 s. A detailed LA geometry was acquired with the mapping catheter and anatomical landmarks were identified and annotated. The array was not moved after geometry creation to avoid distortion of the isopotential maps[12] and the distance between the centre of the MEA balloon and the LA endocardial wall did not exceed 4 cm. Reconstructed virtual AF electrograms (VEGM) projected to the LA surface were collected during steady state in AF over a 5 minute interval. Following this, the MEA was removed and AF ablation proceeded as per standard practice.

Non-contact Mapping

NCM relies on the concept of acquiring simultaneous endocardial electrical activity of the entire cavity without contact between the endocardium wall and electrodes from the MEA.[12, 13] The technique of using NCM with the MEA has previously been described and

validated in published literature, in the context of sinus rhythm as well as arrhythmia in humans.[14-17] Estimation of DF via spectral analysis from NCM has been shown to be very well correlated (agreement in approximately 95% of cases) with DF estimation via spectral analysis from contact mapping for both PAF and persAF.[18, 19]

Signal Processing

VEGMs were sampled at 1200 Hz and high-pass filtered at 1 Hz. No further filtering was applied to the signals to preserve signal integrity and low frequency components.[19] The VEGMs were exported in consecutive time segments for off-line analysis of high density left atrial maps, consisting of 2048 points (a matrix of 32x64 spatial points) of simultaneous data per patient.

VEGMs are affected by the presence of ventricular far-field activity[19] even for areas distant from the mitral valve, [20] which can lead to distortion of results. Hence QRS-T subtraction was performed using a recently validated algorithm[20] to remove far-field ventricular influence. Briefly, the QRS onset and T wave end were segmented on the ECG (highlighted in purple in Figure 1) and their respective positions were projected onto the VEGMs. A template of the ventricular influence for each individual VEGM was then calculated. The template used for cancellation and the resulting signal free from ventricular influence are also shown in Figure 1.

After carrying out ventricular cancellation of the VEGMs, spectral analysis was performed on each of the 2048 points, using Fast Fourier Transform (FFT) with a Hamming window to produce high density 3D DF maps.[21] Segments of 4 s were used with sequential windows producing a 50% overlap (by shifting forward by 2 s) during FFT analysis. Zero padding was applied to improve the identification of spectral peaks. Although zero-padding does not

increase the spectral resolution (i.e. the ability to resolve close spectral peaks) it does interpolate the spectral estimates[22], improving the ability to pinpoint the peak power of the DF - to 0.05 Hz in this case. DF was defined as the frequency with highest power within 4 Hz to 12 Hz.

Temporal DF Analysis

Temporal DF Stability Analysis

For the purpose of assessing temporal stability of DF, we compared the DF of all VEGMs between consecutive time windows (at 2 s intervals), to assess if the DF remained within a defined threshold of ±0.25 Hz or ±0.50 Hz compared to the DF obtained from the first FFT window of the segment (Figure 2). Points whose DF values remained within these thresholds at each time segment were deemed temporally 'stable' (assessed over a period of up to 1 minute) and the resultant DFs were derived by averaging those DF values. If the DF wandered beyond the pre-defined threshold over time, the frequency value was deemed 'unstable' after that particular instant and no longer considered. The total proportion of 'stable' points, as defined by the above criteria, was plotted over time for assessment of temporal stability (Figure 3).

DF Reappearance Analysis

After identifying that DF was not consistently stable over time both for individual recordings (Figure 2B-D) and also by the total proportion of simultaneous recordings of each individual patient (Figure 3 and table 2), further analysis on DF behaviour was performed to investigate if DF values show any temporal repetition or spatial 'reappearance', so as to quantify the presence of any potential DF partial 'periodicity'. This was done by using the first DF value

from each point of interest as a reference, which was then compared with the DF values from the same location while moving forward in time at 2 s intervals (see Figure 4A for illustration). The proportion of DF points falling within the thresholds of ±0.25 or ±0.50 Hz compared to their corresponding reference DF value was plotted over time and defined as DF reappearance points. The time (in seconds) corresponding to any partial 'periodicity' or 'reappearance' of the overall DF behaviour was assessed by spectral estimation of the signal created by counting the number of points that fall within the specified thresholds (±0.25 or ±0.50 Hz of reference DF value) at the same position along time. This is termed the DF reappearance interval. In addition, the impact of applying different FFT window lengths (from 4s to 10s) to identify the DF reappearance was also investigated.

Spatiotemporal Analysis

Highest DF areas Trajectory

To track the behaviour of highest DF areas (HDFAs), the region in the 3D NCM with the highest DF value was identified for each time segment, together with its neighbouring sites, which contained DF values within 0.25 Hz of the highest DF (Figure 5A). This would produce an area consisting of a collection of points that reflect average regional activity, to minimise the effect of isolated high DF sites. The boundary of this area was highlighted to produce an area representative of a maximum DF 'cloud' at that particular instant. The centre of gravity (CG) for the cloud was then identified by averaging the coordinate positions of each point in the cloud, weighted by their respective DF values. [23] These CG points were obtained for each 4 s FFT window and tracked at 2 s intervals over a period of 1 minute to produce a total of 29 sequential CGs, so as to produce a HDFA trajectory map (see Figure 5).

Statistical analysis

All continuous variables are expressed as mean ± standard deviation. Normally distributed data were analysed using paired and unpaired Student's t-test. Categorical data were analysed using Chi squared or Fisher's exact test.

Results

Eight patients with symptomatic drug-refractory persAF were included in this study. A total of 16384 VEGMs and 232 sequential DF maps were analysed. Patients' characteristics are summarised in Table 1.

Temporal Stability analysis

Sequential analysis of individual VEGMs and global DF maps revealed a general lack of temporal DF stability throughout, although periods of apparent stability were also observed (illustrative examples of sequential DF over time from single VEGMs are shown in Figure 2A-B). Approximately 60% of the VEGMs of all patients lost stability in the first 2 s when analysed using the 0.25 Hz threshold and 40% lost stability in the first 2 s using the 0.5 Hz threshold. Analysis of longer segments of continuous recording (Figures 2C-D) demonstrated DF values fluctuating beyond defined thresholds of stability, even when it may have appeared stable initially.

For each patient the overall percentage of stable DF points measured against both thresholds relative to initial DF at those points showed an exponential pattern of loss of stability within the first few seconds (Figures 3). The time constants of the best-fit exponential curves for both thresholds are presented in Table 2, which provides an assessment of how rapidly the DF loses temporal stability. The means of the time constants

for the exponential decay when applying the ±0.25 Hz and ±0.5 Hz thresholds were 3.1±1.4 s and 7.7±3.1 s respectively.

Reappearance of the DF

Although DF in persAF patients was not stable over time for both individual (Figure 2 B-D) and simultaneous high density recordings (Figure 3), individual analysis of VEGMs revealed episodes suggestive of repetition or reappearance of DF over time, where DF loses temporal stability, only to return to a value very close to that of the initial DF (Figure 2B-D). This can be readily appreciated by observing sequential high density non-contact DF maps (Figure 4). The first 3D DF frame (time = 4 s) shows the discrete highest DF area with DF around 7.8 Hz (coloured orange) localized at the LA roof. The frequency of the neighbour DF areas were 6.7 Hz close to the right superior PV (RSPV, top, light green), 7.1 Hz at the posterior wall (PW, right, yellow) and 6.1 Hz at the anterior wall (AW, bottom, cyan). A few seconds later, at time 10 s, the area over which the highest DF was seen was dramatically reduced in size when compared with the previous frame and its frequency value was also reduced (to about 7.3 Hz, lighter orange – yellow colour). The location of the highest DF had shifted over time from the LA roof to closer to the RSPV and the value reduced. In the third frame, the highest DF area reappears at the LA roof in DF value and 'cloud' area with the DF value around 7.65 Hz. Its DF neighbours areas have their DF values at 7.1 Hz (right-top), 6.1 Hz (cyan, left) and around 4 Hz in the remaining LA areas. The behaviour of the HDFA site has changed over time. The small area that contains DF values which were 'similar' over the 14 s period of the 3 frames would agree with the aforementioned decay behaviour of DF over time whereby a small proportion of the sites would have 'stable' DF within this time period using the 2 thresholds (see example in Figure 3), but no longer remained stable beyond around 30 s.

DF reappearance analysis as described earlier was performed to quantify the observed behaviour by obtaining the DF reappearance interval (see Table 2). The DF reappearance interval was similar when comparing short (20 s) and longer (5 minutes) recordings in one patient; 6.9 vs. 6.5 s (0.25 Hz threshold) and 9.4 vs. 10.7 s (0.5 Hz threshold) respectively (Table 2 Patient 5). However, when we changed the FFT window length from 4 s to 7 s and then 10 s, we could see an apparent change of this periodic behaviour. When the window length is increased, a temporal averaging process happens giving a false idea of 'stability'.

Highest DF area and its trajectory

Having seen the dynamic behaviour of DF and its lack of temporal stability, we proceeded with the tracking of HDFAs at each time point by plotting the trajectory of its CG, so as to determine its spatial characteristics. This revealed 3 patterns of behaviour (Figure 5):

i. Type I (Local activity) – CG propagation trajectory area (total area encompassed by the trajectory) < 5% of the LA area over consecutive time frames;

ii. Type II (Cyclical) – CG propagation trajectory area > 5% of LA area but showing a trajectory that returns to the vicinity of at least one of its earlier CG sites over time;

iii. Type III (Chaotic) – CG propagation trajectory area > 5% of LA area with a random pattern of movement and no overlap of CGs over consecutive time frames.

A total of 7 local activity events (mean time per event: 2.86±1.07 s), 15 cyclical events (5.07±1.49 s), and 2 chaotic events (4.50±1.91 s) were identified over a 20 s segment analysis in all patients. When we extended the analysis to 1 minute, the number of events increased respectively to 24, 54 and 6. The mean times spent in each separate event were similar between 20 s and 1 minute analyses (2.86±1.07 s *vs.* 2.83±1.55 s, p= 0.9701 for local

activity; 5.07±1.49 s *vs.* 5.14±2.16 s, p= 0.2620 for cyclic activity; and 4.5±1.91 s *vs.* 4.60±0.97 s, p= 0.29 for chaotic activity). The proportion of time spent in each pattern of behaviour is presented in Table 3. Cyclical activity was the most prevalent behaviour observed, followed by local and then chaotic activity. All except one patient (patient 8) had cyclical activity as the predominant behaviour over 20 s and 1 minute. The DF trajectory showed a concentration of HDFAs in the roof and around the pulmonary veins. The mean HDFA value was 7.29±0.71 Hz.

Discussion

Using NCM analysis of individual VEGMs, we have demonstrated that DF is not temporally stable during persAF, although reappearance of DF values can occur at times. By using a novel method of tracking the movement of HDFAs, we have also shown the presence of distinct localized, cyclical and chaotic behaviour spatially.

Significance of DF mapping

Previous research had suggested that targeting sites of highest DF may be important for catheter ablation.[5, 6] It had also been demonstrated that ablation reduces the DF of AF electrograms[7, 24, 25] and that a decrease in DF may be associated with a more favourable outcome.[5] However, DF-guided ablation has not been widely adopted and published data using this approach is limited, partly because its clinical significance is not fully understood.

Spatiotemporal stability

Spatiotemporal stability of DF sites has previously been studied by other authors. Schuessler *et al.*[26] carried out epicardial contact mapping (CM) of the atria of patients undergoing open

heart surgery while in AF and found that the location of the HDFAs were variable and did not remain fixed in a significant proportion of the patients. Sanders *et al*.[4] reported that DF values from contact electrograms were stable over time, although this observation was limited by the sequential, point-by-point mapping technique used. A study comparing simultaneous multipolar CM with sequential mapping[27], found that potential AF driver sites were more readily identified via FFT analysis in the former technique. Two recent studies (one using NCM[8] and another using multipolar catheter for CM[28]) also concluded that DF lacked temporal stability. There is therefore emerging evidence, including results from our study, that strongly support the notion that DF behaviour is dynamic and should be analysed ideally with simultaneous multipolar CM or NCM techniques.

As observed in our study, DF of individual VEGMs was largely temporally unstable, although there appeared to be transient episodes of stable DF, as well as a degree of reappearance of DF activity over time, mostly within 10s. It is therefore possible that apparent DF stability could be explained by: 1) the use of a single segment for the DF analysis (producing a "snapshot" and not the full sequence of DF behaviour); 2) choice of the length for the segments for DF analysis that is too short and using too few segments, resulting in the opportunistic capture of transiently stable DF signals; 3) reappearance behaviour causing the illusion of stability when DF values are averaged or collected sequentially; 4) choice of long FFT window segments, which would improve spectral resolution at the cost of reducing temporal resolution, effectively 'blurring the video'.

3D Trajectory mapping

Localized and cyclical DF cloud activity accounted for most of the observed behaviour in the patients we studied. In fact the data show considerable repetitive and cyclical behaviour in

analyses of DF trajectory, accounting for almost 64% of the time (table 3) while spatial localization within 5% of the left atrial area occurred in about 27% of all the cases in this study. While localized activity seen in our study could theoretically be attributed to a stable rotor or micro-reentrant behaviour, the finding of cyclical DF activity is not as intuitive. Using optical mapping of AF in sheep hearts, Skanes *et al.*[29] demonstrated the presence of periodic activity in the atrium, with local DF showing good correlation with DF of the atrium globally. The periodic activation was noted to be transient in most cases, although the patterns of periodicity tended to reappear over time. This was an interesting observation which is similar to what was seen in our study, where there was a predominance of a cyclical behaviour identified when the HDFAs were tracked. The reasons for this are not immediately clear. Potential explanations include interference by other competing activation sources, failure of local atrial tissue to sustain the same frequency of activation for long periods, or even potential migratory behaviour of rotors, if indeed present. A subsequent study using the same sheep AF model[30] however, showed the presence of spatiotemporally stable rotor behaviour persisting for up to 30 minutes. This would appear to support an earlier animal study by Schuessler *et al.*[31], where multiple re-entrant circuits were found to stabilise to a single, stable re-entrant circuit when AF became sustained over time. It has to be noted, however, that episodes of AF in this and the earlier study were experimentally induced and may not necessarily reflect the clinical reality of persAF in human hearts.

Characterising dynamic electrical activation in the search for 'rotors' in human AF has continued to be an area of keen research interest. Using epicardial mapping of patients undergoing open heart surgery, Sahadevan *et al.*[32] found evidence for potential driver sites,

producing fibrillatory conduction in the atria of most of the subjects studied. Three recent studies into the mapping of human AF however, have not been able to demonstrate convincing rotor activity.[8,33,34] Using a novel computational mapping technique, Narayan *et al.*[9] found evidence for focal impulses and rotor activation patterns during AF in human subjects. An initial series of patients undergoing AF ablation guided by these maps, in addition to conventional ablation, have shown favourable outcomes compared to conventional ablation alone.[10]

Significance of findings and clinical implications

Our results provide further insight into the potential mechanisms of persAF. Current mechanistic concepts include single re-entry with fibrillatory conduction (i.e. rotor driven) and the multiple wavelet hypotheses. Our findings show agreement with both proposed mechanisms. We observed a predominance of local and cyclical maximal DF activity, which may imply a higher proportion of rotor driven episodes, although the lack of spatiotemporal DF stability makes it unlikely that AF is being primarily sustained by anatomically stable high DF sites. The presence of a cyclical pattern does suggest a certain extent of spatial consistency and it may be important to characterise this in each individual patient to help guide ablation strategy. Chaotic maximal DF propagation seen in our study would be analogous to multiple wavelet activity. It is interesting to note that in our study, all 3 patterns of behaviour can be observed in the same individual patient over time.

It is likely that more than one mechanism may be involved in AF perpetuation at different stages of the arrhythmia history in any given individual. Depending on the extent of electromechanical remodelling and autonomic influence, a particular mechanism may predominate, resulting in different subtypes of persAF. This could explain why an

anatomical-based ablation strategy tends to produce only modest results for persAF. A tailored ablation approach should therefore be considered for each individual case, provided that effective real-time, high resolution DF mapping can be performed.

Limitations

This was a study involving a small number of patients, as our main objective was to describe the DF behaviour using high-density NCM of persAF. Electrogram analysis was restricted only to the LA, hence any potential contributions from the right atrium were not studied. We acknowledge that some of the patients in the study were taking amiodarone which could potentially affect the DF of VEGMs. Nevertheless, our observations from the study would still be applicable to real-world practice, where patients are not infrequently put on this drug leading up to ablation. In addition, we have focused the current study on understanding the spatio-temporal behaviour of DF during persAF. Previously, as in the current study, analysis of DF behaviour required a rather laborious process of exporting the continuous 2048 VEGMs from the geometry which could only be done offline. With the purchase of more powerful computer, including the employment of parallel processing[21], we are now in a position to perform the analysis in real-time, which makes it possible to provide clinically useable data to guide strategy during the ablation procedure.

Conclusions

Using high density NCM of the LA, we have demonstrated that DF of AF electrograms lack spatiotemporal stability, hence targeting sites of peak DF from a single time frame is unlikely to be a reliable ablation strategy. Tracking of the CGs of the HDFAs revealed the presence of localized, cyclical and chaotic patterns of propagation, with more than 90% of all cases

presenting either a localized (27%) or cyclical (64%) behaviour. While in most of the places DF changed over time, this combination of localized and cyclical activity hints at a potentially non-random temporally periodic behaviour, thereby providing further insight into potential mechanisms underlying persAF. This would be of particular significance if an ablation approach to target DF locations is taken. Studies should be performed to assess the efficacy of using dynamic 3D DF maps to aid ablation strategy for patients with persAF.

Acknowledgement

This study is part of the research portfolio supported by the National Institute for Health Research Leicester Cardiovascular Biomedical Research Unit.

Author contributions

JL Salinet: Concept/design study, Data analysis/interpretation of results, Drafting manuscript, Critical revision of manuscript, Statistics, Funding secured from CNPq and 'off-line' Data collection.

JH Tuan: EP study and data collection, interpretation of results, drafting manuscript as joint first author.

AJ Sandilands: EP study, interpretation of results.

PJ Stafford: EP studies and ablation procedures, Interpretation of results, Critical revision of manuscript.

FS Schlindwein: Data analysis/interpretation of results, Critical revision of manuscript. Funding secured from IPEM, Santander and University of Leicester.

G. André Ng: EP studies and ablation procedures, Interpretation of results, Critical revision of manuscript, Funding secured from St. Jude Medical Inc.

References

1. Cappato R, Calkins H, Chen SA, Davies W, Iesaka Y, Kalman J, Kim YH, Klein G, Natale A, Packer D, Skanes A, Ambrogi F, Biganzoli E: Updated worldwide survey on the methods,

efficacy, and safety of catheter ablation for human atrial fibrillation. Circ Arrhythm Electrophysiol 2010; 3:32-38.

2. Brooks AG, Stiles MK, Laborderie J, Lau DH, Kuklik P, Shipp NJ, Hsu LF, Sanders P: Outcomes of long-standing persistent atrial fibrillation ablation: a systematic review. Heart Rhythm 2010; 7:835-846.

3. Skanes A, Mandapati R, Berenfeld O, Davidenko JM, Jalife J: Spatiotemporal periodicity during atrial fibrillation in the isolated sheep heart. Circulation 1998; 1236-1248.

4. Sanders P, Berenfeld O, Hocini M, Jaïs P, Vaidyanathan R, Hsu LF, Garrigue S, Takahashi Y, Rotter M, Sacher F, Scavée C, Ploutz-Snyder R, Jalife J, Haïssaguerre M: Spectral analysis identifies sites of high-frequency activity maintaining atrial fibrillation in humans. Circulation 2005; 112:789-797.

5. Yoshida K, Chugh A, Good E, Crawford T, Myles J, Veerareddy S, Billakanty S, Wong WS, Ebinger M, Pelosi F, Jongnarangsin K, Bogun F, Morady F, Oral H: A critical decrease in dominant frequency and clinical outcome after catheter ablation of persistent atrial fibrillation. Heart Rhythm 2010; 7:295-302.

6. Atienza F, Almendral J, Jalife J, Zlochiver S, Ploutz-Snyder R, Torrecilla EG, Arenal A, Kalifa J, Fernández-Avilés F, Berenfeld O: Real-time dominant frequency mapping and ablation of dominant frequency sites in atrial fibrillation with left-to-right frequency gradients predicts long-term maintenance of sinus rhythm. Heart Rhythm 2009; 6:33-40.

7. Tuan J, Jeilan M, Kundu S, Nicolson W, Chung I, Stafford PJ, Ng GA: Regional fractionation and dominant frequency in persistent atrial fibrillation: effects of left atrial ablation and evidence of spatial relationship. Europace 2011; 13:1550-6.

8. Jarman JWE, Wong T, Kojodjojo P, Spohr H, Davies JE, Roughton M, Francis DP, Kanagaratnam P, Markides V, Davies DW and Peters NS: Spatiotemporal behaviour of high DF during paroxysmal and persistent atrial fibrillation in the human left atrium. Circ Arrhythm Electrophysiol 2012; 5:650-8.

9. Narayan SM, Krummen DE, Rappel W-J: Clinical mapping approach to diagnose electrical rotors and focal impulse sources for human atrial fibrillation. J Cardiovascular Electr. 2012; 23:447-454.

10. Narayan SM, Krummen DE, Shivkumar K, Clopton P, Rappel W-J, Miller JM: Treatment of atrial fibrillation by localized sources: CONFIRM (Conventional Ablation for Atrial Fibrillation with or without Focal Impulse and Rotor Modulation) Trial. J Am Coll Cardiol 2012; 60:628-636.

11. Fuster V, Ryden LE, Cannom DS, Crijns HJ, Curtis AB, Ellenbogen KA, Halperin JL, Heuzey JYL, Kay GN, Lowe JE, Olsson SB, Prystowsky EN, Tamargo JL, Wann S, Smith Jr. SC, Jacobs AK,

Adams CD, Anderson JL, Antman EM, Hunt SA, Nishimura R, Ornato JP, Page RL, Riegel B, Priori SG, Blanc JJ, Budaj A, Camm AJ, Dean V, Deckers JW, Despres C, Dickstein K, Lekakis J, McGregor K, Metra M, Morais J, Osterspey A, Zamorano JL: ACC/AHA/ESC 2006 Guidelines for the management of patients with atrial fibrillation: a report of the American College of Cardiology/American Heart Association Task Force on Practice Guidelines and the European Society of Cardiology Committee for Practice Guidelines (writing committee to revise the 2001 guidelines for the management of patients with atrial fibrillation): Developed in collaboration with the European Heart Rhythm Association and the Heart Rhythm Society." Circulation 2006; 114:700-752.

12. Chinitz LA, Sethi JS: How to perform noncontact mapping. Heart Rhythm 2006; 3:120-123.

13. Sy RW, Thiagalingam A, Stiles MK: Modern electrophysiology mapping techniques. Heart, Lung and Circulation 2012; 21:364-375.

14. Schilling RJ, Peters NS, Davies W: Simultaneous endocardial mapping in the human left ventricle using a noncontact catheter - comparison of contact and reconstructed electrograms during sinus rhythm. *Circulation* 1998; 9:887-898.

15. Schilling RJ, Peters NS, Goldberger J, Kadish AH, Davies DW: Characterization of the anatomy and conduction velocities of the human right atrial flutter circuit determined by noncontact mapping. *JACC* 2001; 38:385-393.

16. Schilling RJ, Peters NS, Davies DW: Feasibility of a noncontact catheter for endocardial mapping of human ventricular tachycardia. *Circulation* 1999; 99:2543-2552.

17. Hindricks G, Kottkamp H: Simultaneous noncontact mapping of left atrium in patients with paroxysmal atrial fibrillation. *Circulation* 2001; 104:297-303.

18. Lin Y, Higa S, Kao T, Tso H-W, Tai C-T, Chang S-L, Lo L-W, Wongcharoen W, Chen S-A: Validation of the Frequency Spectra Obtained from the Noncontact Unipolar Electrograms During Atrial Fibrillation. *J Cardiovasc. Electr* 2007; 18:1147-1153.

19. Gojraty S, Lavi N, Valles E, Kim SJ, Michele J, Gerstenfeld EP: Dominant frequency mapping of atrial fibrillation: comparison of contact and noncontact approaches. J Cardiovasc Electr 2009; 20:997-1004.

20. Salinet Jr JL, Madeiro JPV, Cortez PC, Stafford P, Ng GA, Schlindwein FS: Analysis of QRS-T subtraction in unipolar atrial fibrillation electrograms. "In press" Med Biol Eng Comput 2013 DOI: 10.1007/s11517-013-1071-4.

21. Salinet Jr JL, Oliveira GN, Vanheusden FJ, Comba JLD, Ng GA, Schlindwein FS: Visualizing Intracardiac Atrial Fibrillation Electrograms Using Spectral Analysis. Comput Sci Eng 2013; 15:79-87.

22. Marple SJ. Digital Spectral Analysis, New Jersey: Prentice-Hall, Inc: 1987; pp 43-44.

23. Assis AKT. Archimedes, the Center of gravity, and the first law of mechanics. 2nd ed. Montreal: C. Roy Keys Inc.; 2010: pp.185-190.

24. Takahashi Y, Sanders P, Jaïs P, Hocini M, Dubois R, Rotter M, Rostock T, Nalliah CJ, Sacher F, Clémenty J, Haïssaguerre M: Organization of frequency spectra of atrial fibrillation: relevance to radiofrequency catheter ablation. J Cardiovasc Electr 2006; 17:382-388.

25. Lemola K, Ting M, Gupta P, Anker JN, Chugh A, Good E, Reich S, Tschopp D, Igic P, Elmouchi D, Jongnarangsin K, Bogun F, Pelosi F Jr, Morady F, Oral H: Effects of two different catheter ablation techniques on spectral characteristics of atrial fibrillation. *J Am Coll Cardiol* 2006; 48:340-348.

26. Schuessler RB, Kay MW, Melby SJ, Branham BH, Boineau JP, Damiano RJ: Spatial and temporal stability of the dominant frequency of activation in human atrial fibrillation. *J Electrocardiol* 2006; 39:S7-S12.

27. Krummen DE, Peng KA, Bullinga JR, Narayan SM: Centrifugal gradients of rate and organization in human atrial fibrillation. *Pacing Clin Electrophysiol* 2009;32:1366-1378.

28. Habel N, Znojkiewicz P, Thompson N, Müller JG, Mason B, Calame J, Calame S, Sharma S, Mirchandani G, Janks D, Bates J, Noori A, Karnbach A, Lustgarten DL, Sobel BE, Spector P: The temporal variability of DF and CFAEs constrains the validity of sequential mapping in human atrial fibrillation. *Heart Rhythm* 2010;7:586-593.

29. Skanes AC, Mandapati R, Berenfeld O, Davidenko JM, Jalife J: Spatiotemporal periodicity during atrial fibrillation in the isolated sheep heart. *Circulation* 1998;98:1236-1248.

30. Mandapati R, Skanes A, Chen J, Berenfeld O, Jalife J: Stable microreentrant sources as a mechanism of atrial fibrillation in the isolated sheep heart. *Circulation* 2000;101:194-199.

31. Schuessler RB, Grayson TM, Bromberg BI, Cox JL, Boineau JP: Cholinergically mediated tachyarrhythmias induced by a single extrastimulus in the isolated canine right atrium. *Circ Res* 1992;71:1254-1267.

32. Sahadevan J, Ryu K, Peltz L, Khrestian CM, Stewart RW, Markowitz AH, Waldo AL: Epicardial mapping of chronic in patients: preliminary observations. *Circulation* 2004;110:3293-3299.

33. de Groot NMS, Houben RPM, Smeets JL, Boersma E, Schotten U, Schalij MJ, Crijns H, Allessie MA: Electropathological substrate of longstanding persistent atrial fibrillation in patients with structural heart disease: epicardial breakthrough. *Circulation* 2010;122:1674-1682.

34. Cuculich PS, Wang Y, Lindsay BD, Faddis MN, Schuessler RB, Damiano RJ Jr, Li L, Rudy Y: Noninvasive characterization of epicardial activation in humans with diverse atrial fibrillation patterns. *Circulation* 2010;122:1364-1372.

Tables

Table 1. Patients' characteristics.

	n=8
Male, n	8
Age, y	47 ± 10
AF duration, mo	34± 25
Hypertension, n	2
LV function, n	
EF ≥55%	5
EF 45-54%	2
EF 36-44%	-
EF≤35%	1
LA Size, mm	48 ± 6
On amiodarone, n	3

AF indicates atrial fibrillation; LV, left ventricular; EF, ejection fraction; LA, left atrial.

Table 2. Overall DF temporal stability (time constant) and DF reappearance analyses of the 2048 simultaneous VEGMs calculated for both DF thresholds (0.25 Hz and 0.5Hz).

	Time Constant (s)		DF Reappearance Interval (s)	
	0.25 Hz	**0.5 Hz**	**0.25 Hz**	**0.5 Hz**
Patient 1	1.2	2.5	9.8	8.5
Patient 2	2.3	4.2	5.8	5.0
Patient 3	2.6	8.7	7.8	7.7
Patient 4	1.6	11.1	11.7	7.8
Patient 5	4.2	9.8	6.9	9.4
Patient 6	4.3	10.1	10.8	7.4
Patient 7	4.4	6.2	5.5	6.9
Patient 8	3.8	9.4	5.8	8.5
Mean (SD)	3.1 (1.4)	7.7 (3.1)	8.0 (2.4)	9.8 (6.5)

SD indicates standard deviation

Table 3. Percentage of the time spent on each trajectory pattern for both short term (20 s) and long term (1 min) analysis during HDFAs trajectory propagation.

	Analysis during 20 s				Analysis during 1 min			
	Localized (% of time)	**Cyclical (% of time)**	**Chaotic (% of time)**	**Total (% of time)**	**Localized (% of time)**	**Cyclical (% of time)**	**Chaotic (% of time)**	**Total (% of time)**
Patient 1	0.0	100.0	0.0	100.0	16.6	83.4	0.0	100.0
Patient 2	33.0	67.0	0.0	100.0	30.0	70.0	0.0	100.0
Patient 3	33.0	67.0	0.0	100.0	30.8	61.2	8.0	100.0
Patient 4	0.0	50.0	50.0	100.0	12.5	62.5	25.0	100.0
Patient 5	33.0	67.0	0.0	100.0	27.3	54.7	18.0	100.0
Patient 6	33.0	67.0	0.0	100.0	30.0	60.0	10.0	100.0
Patient 7	33.0	67.0	0.0	100.0	28.5	57.5	14.0	100.0
Patient 8	50.0	25.0	25.0	100.0	40.0	40.0	20.0	100.0
Mean (SD)	26.9 (17.6)	63.8 (20.9)	9.4 (18.6)		27.0 (8.6)	61.2 (12.4)	11.9 (9.1)	

SD indicates standard deviation.

Figure Captions:

Figure 1. Method of ventricular far-field cancellation from VEGMs. The surface ECG is used for QRS-T detection and then a template, based on the VEGM, with onset of QRS (marked with squares) to the end of T wave (marked with circles) is subtracted from the raw VEGMs as described in the methodology section. The frequency spectrum of the raw VEGM signal compared with that after QRS-T subtraction is shown.

Figure 2. Plots of DF over time from single site VEGMs. Examples of apparently stable (A) and unstable (B) DF behaviour in a patient are exhibited. Two longer recordings showing transient stability of DF with subsequent fluctuations over time (C and D).

Figure 3. Sequence of 3D DF maps during AF for one patient and accompanying plot of percentage of stable DF points over time. It can be observed that the number of stable DF points out of 2048 VEGMs decreases with time in an exponential pattern with time constant of 4.24 s and 9.79 s respectively for 0.25 Hz and 0.5 Hz thresholds. The 3D DF maps highlight the sites that remained temporally stable for 2 s, 6 s and 32 s within a threshold 0.25 Hz, with the sites that lost stability greyed out. (Tags for RSPV: green, RLPV: blue, LSPV: brown and LLPV: cyan).

Figure 4. Illustration of the method used for DF reappearance analysis; every DF map within the duration of the recording is compared with a reference DF map within the thresholds of ±0.25 and ±0.5 Hz for each of the 2048 points. This is carried out for every single point and repeated across the entire LA (A); an example of a DF map showing reappearance of DF projected onto its 3D LA geometry (B) and also displayed as a 2D map (C) for better visualisation (at 4 s, 10 s and 18 s). Sites containing the higher DF values (in yellow and orange) at 4s, shifted over time and the DF value reduced, but reappear at 18s (orange areas, for instance). The small area that contains DF values which were ‘similar’ over the 14s

period of the 3 frames would agree with the aforementioned decay behaviour of DF over time whereby a small proportion of the sites would have ‘stable’ DF within this time period using the 2 thresholds (see example in Figure 3), but the DF sites had not remained stable for considerable longer segment episodes duration.

Figure 5. Identification and tracking of the centre of gravity (CG) of the highest DF cloud for a specific time segment (A). 3 types of behaviour were seen: Type 1 - localized (B), Type 2 - cyclical (C) and Type 3 - chaotic (D).

Figure 1

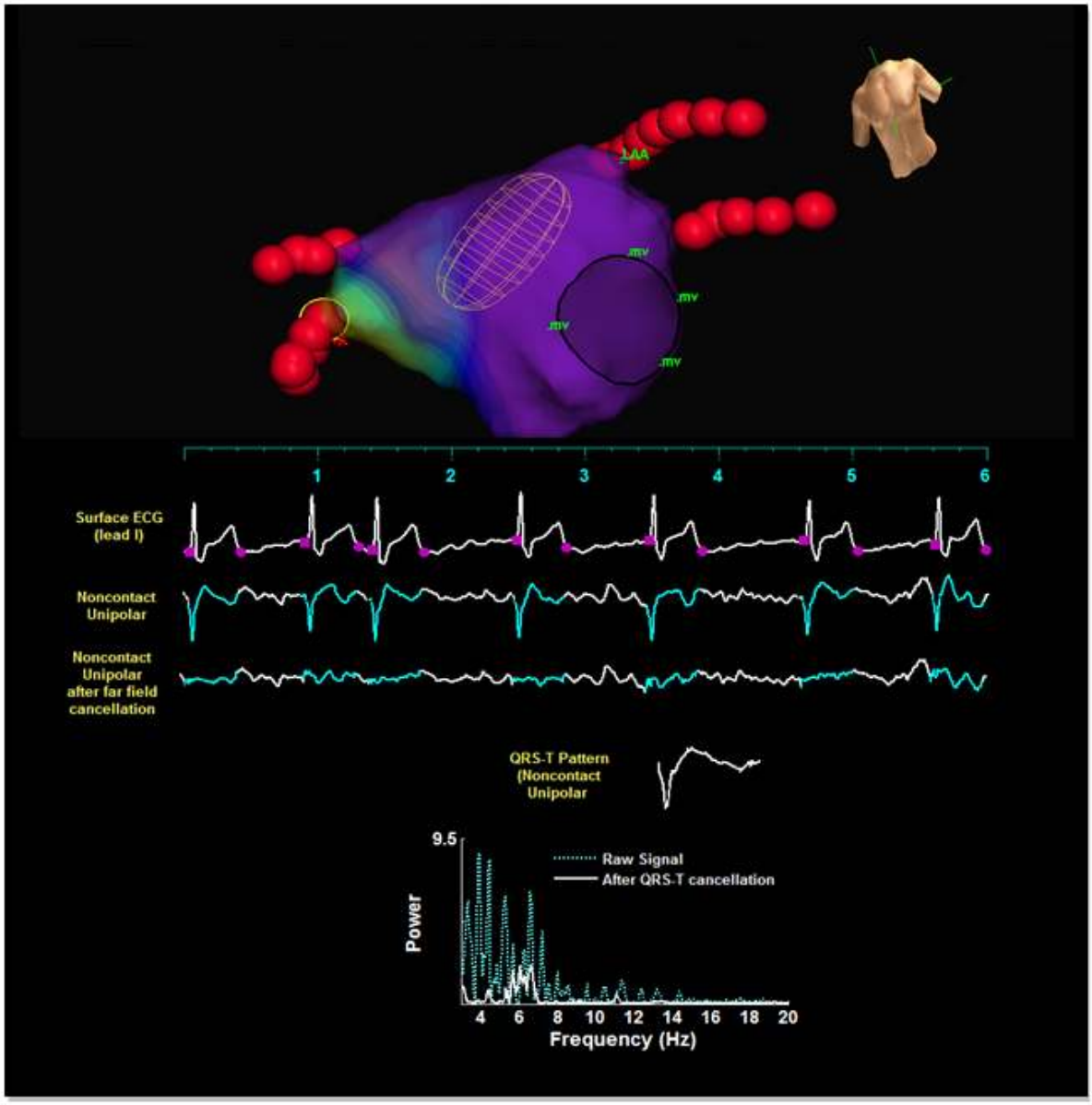
LAA
mv
mv
mv
mv
1
2
3
4
5
6
Surface ECG (lead I)
Noncontact Unipolar
Noncontact Unipolar after far field cancellation
QRS-T Pattern (Noncontact Unipolar
9.5
Power
Raw Signal
After QRS-T cancellation
4
6
8
10
12
14
16
18
20
Frequency (Hz)

Figure 2

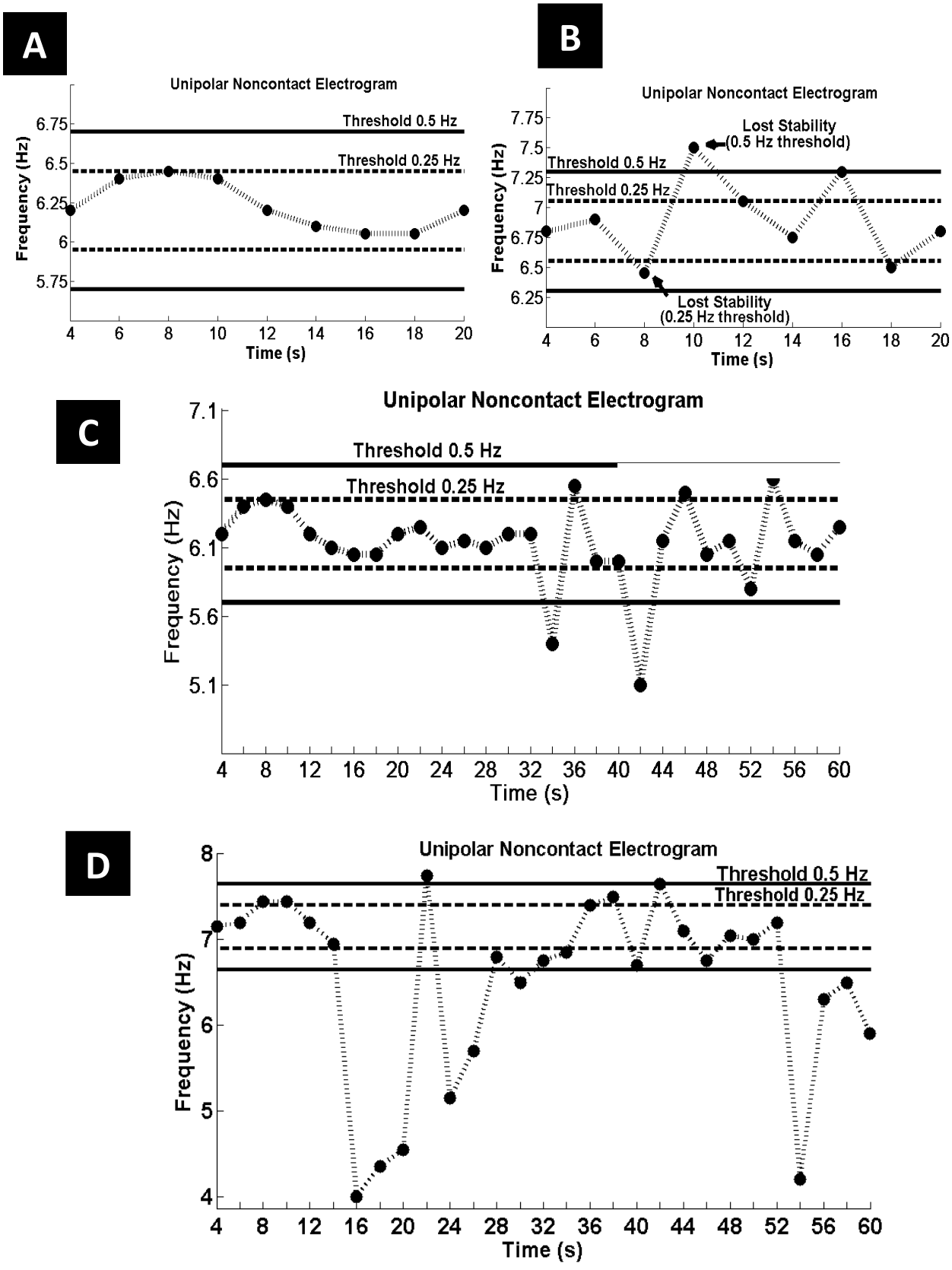
A
Unipolar Noncontact Electrogram
Threshold 0.5 Hz
Threshold 0.25 Hz
Frequency (Hz)
Time (s)
B
Unipolar Noncontact Electrogram
Lost Stability
(0.5 Hz threshold)
Threshold 0.5 Hz
Threshold 0.25 Hz
Lost Stability
(0.25 Hz threshold)
Frequency (Hz)
Time (s)
C
Unipolar Noncontact Electrogram
Threshold 0.5 Hz
Threshold 0.25 Hz
Frequency (Hz)
Time (s)
D
Unipolar Noncontact Electrogram
Threshold 0.5 Hz
Threshold 0.25 Hz
Frequency (Hz)
Time (s)

Figure 3

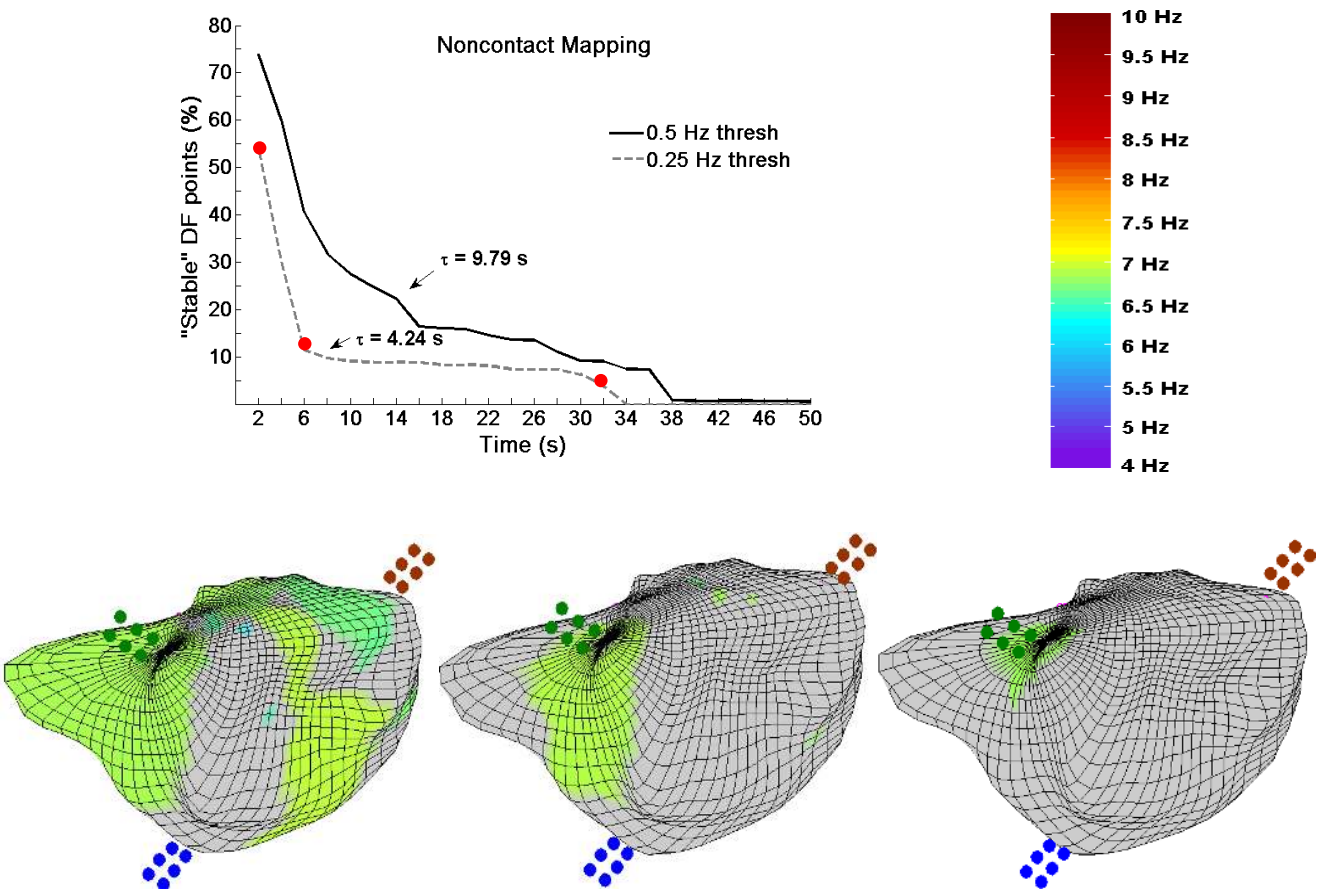
Noncontact Mapping
"Stable" DF points (%)
Time (s)
0.5 Hz thresh
0.25 Hz thresh
τ = 9.79 s
τ = 4.24 s
10 Hz
9.5 Hz
9 Hz
8.5 Hz
8 Hz
7.5 Hz
7 Hz
6.5 Hz
6 Hz
5.5 Hz
5 Hz
4 Hz
Stable for 2 s
Stable for 6 s
Stable for 32 s

Figure 4

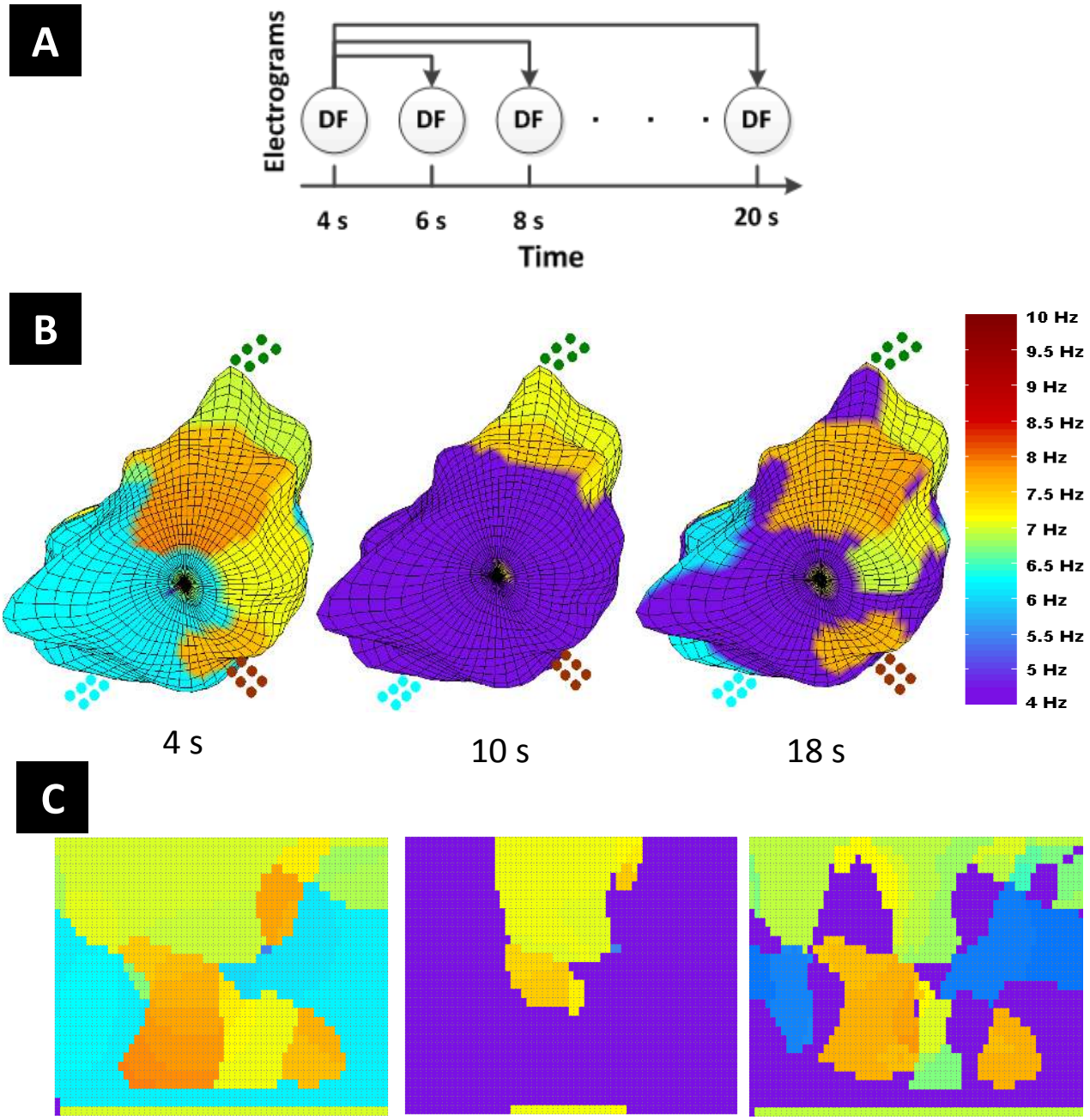
A
Electrograms
DF
DF
DF
DF
4 s
6 s
8 s
20 s
Time
B
10 Hz
9.5 Hz
9 Hz
8.5 Hz
8 Hz
7.5 Hz
7 Hz
6.5 Hz
6 Hz
5.5 Hz
5 Hz
4 Hz
4 s
10 s
18 s
C

Figure 5

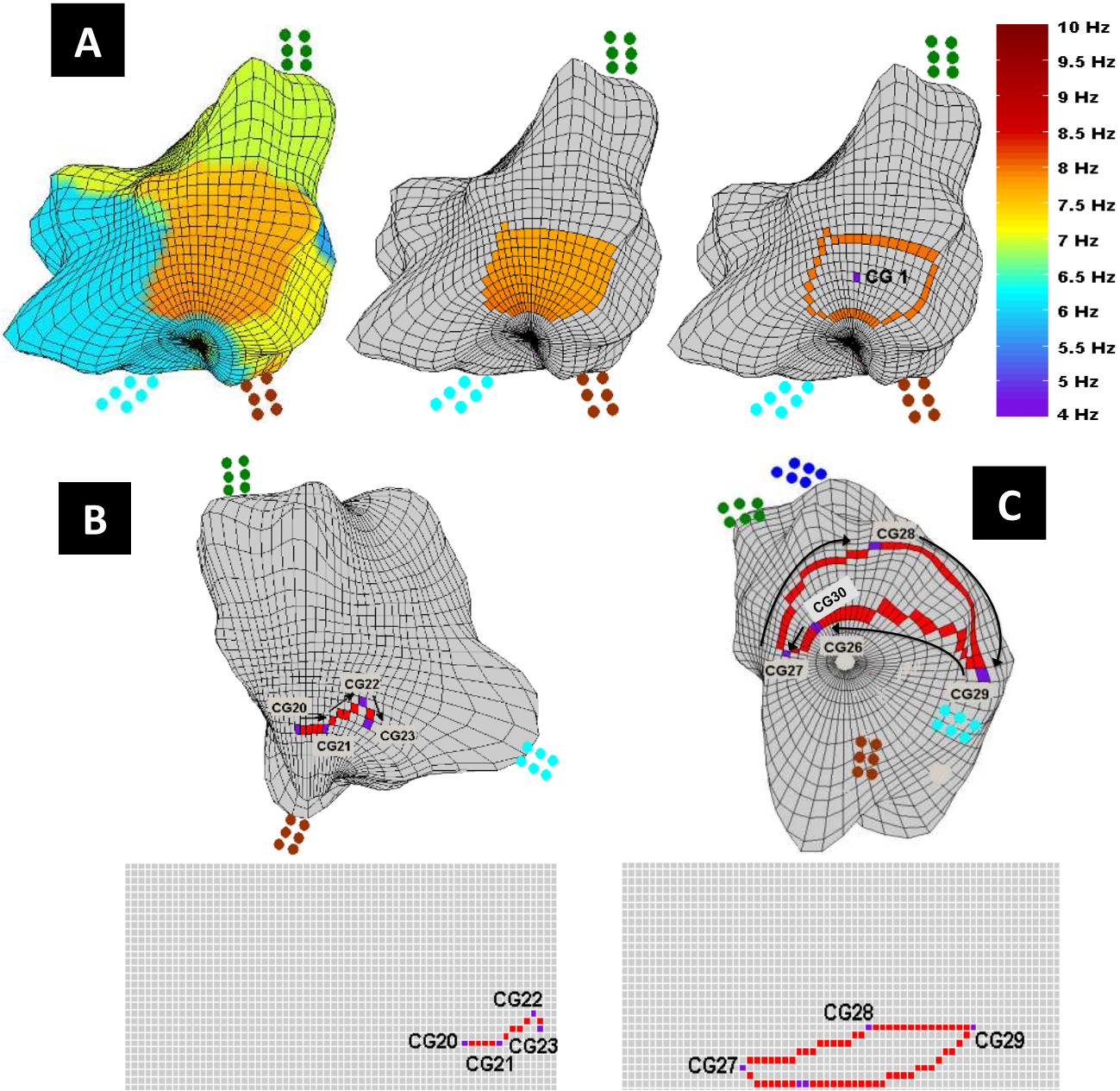
A
10 Hz
9.5 Hz
9 Hz
8.5 Hz
8 Hz
7.5 Hz
7 Hz
6.5 Hz
6 Hz
5.5 Hz
5 Hz
4 Hz
CG 1
B
CG20
CG21
CG22
CG23
C
CG26
CG27
CG28
CG29
CG30
CG22
CG20
CG23
CG21
CG28
CG27
CG29
Localised
Cyclical

Figure 5 (Continued)

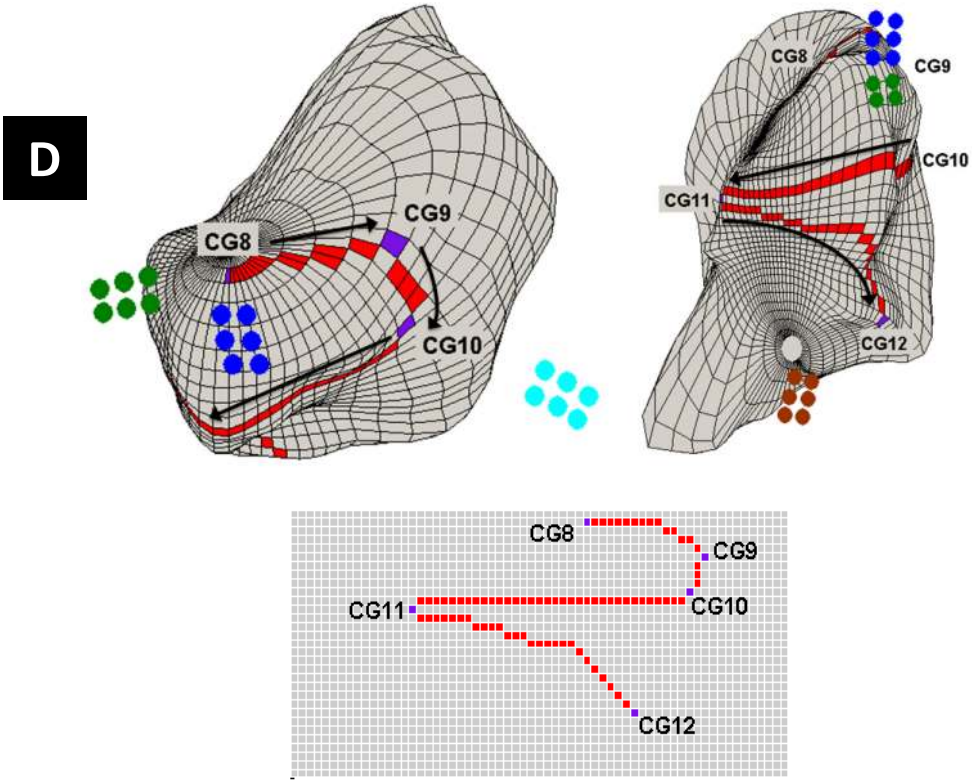

Chaotic

Figures in higher resolution and enlarged

Figure 1

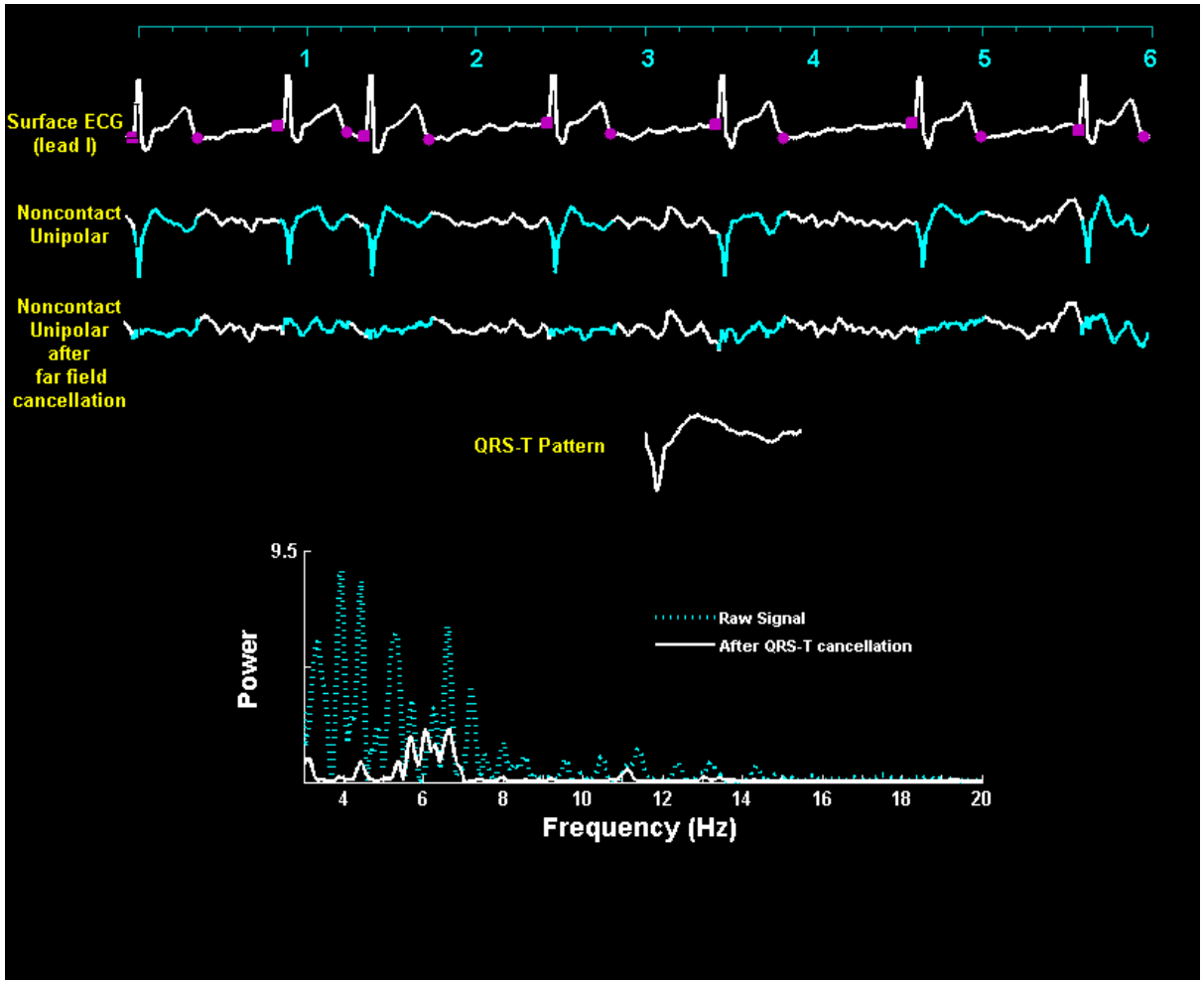
1
2
3
4
5
6
Surface ECG (lead I)
Noncontact Unipolar
Noncontact Unipolar after far field cancellation
QRS-T Pattern
9.5
Power
Raw Signal
After QRS-T cancellation
4
6
8
10
12
14
16
18
20
Frequency (Hz)

Figure 2

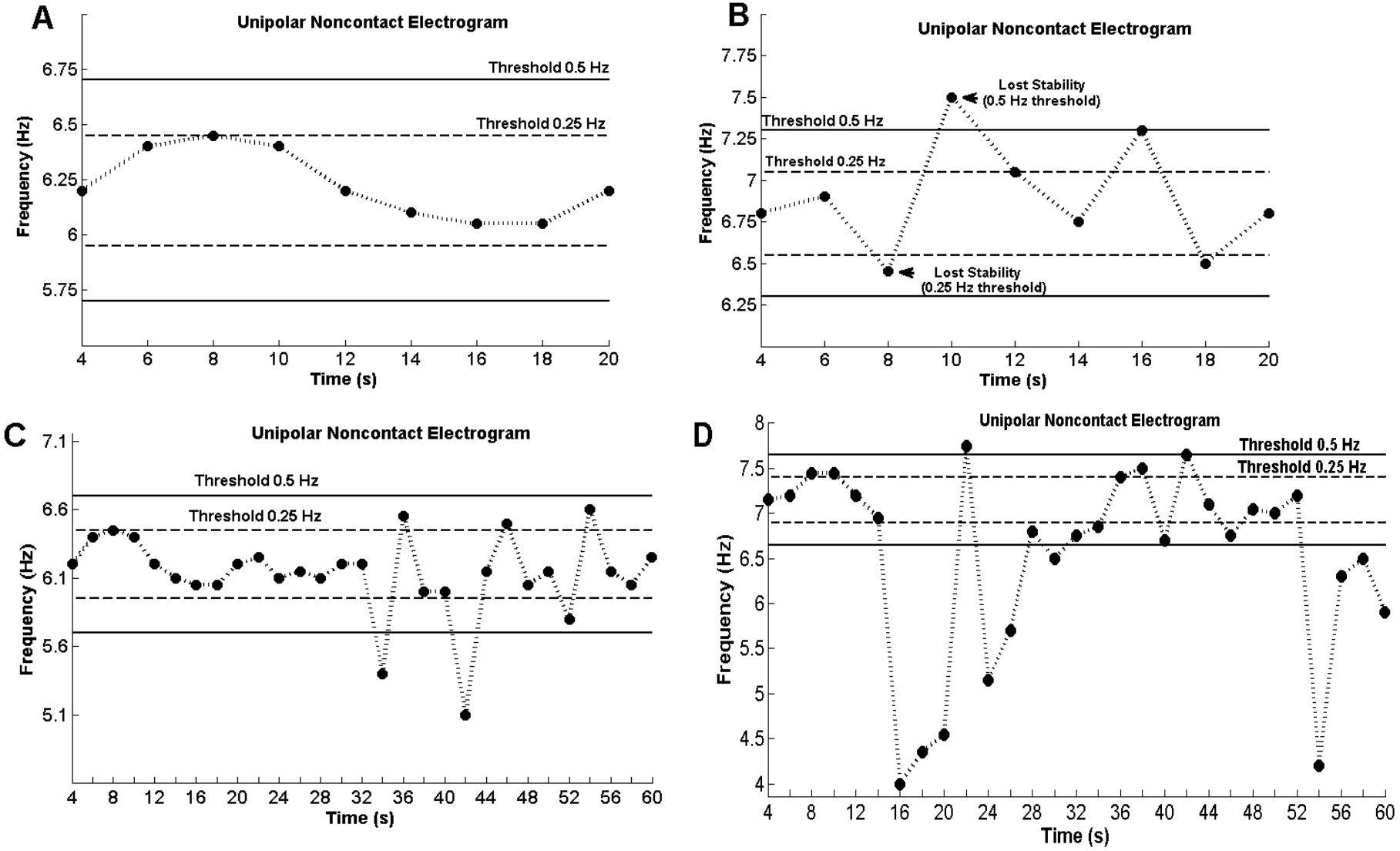
A
Unipolar Noncontact Electrogram
Threshold 0.5 Hz
Threshold 0.25 Hz
Frequency (Hz)
Time (s)
B
Unipolar Noncontact Electrogram
Lost Stability
(0.5 Hz threshold)
Threshold 0.5 Hz
Threshold 0.25 Hz
Lost Stability
(0.25 Hz threshold)
Frequency (Hz)
Time (s)
C
Unipolar Noncontact Electrogram
Threshold 0.5 Hz
Threshold 0.25 Hz
Frequency (Hz)
Time (s)
D
Unipolar Noncontact Electrogram
Threshold 0.5 Hz
Threshold 0.25 Hz
Frequency (Hz)
Time (s)

Figure 3

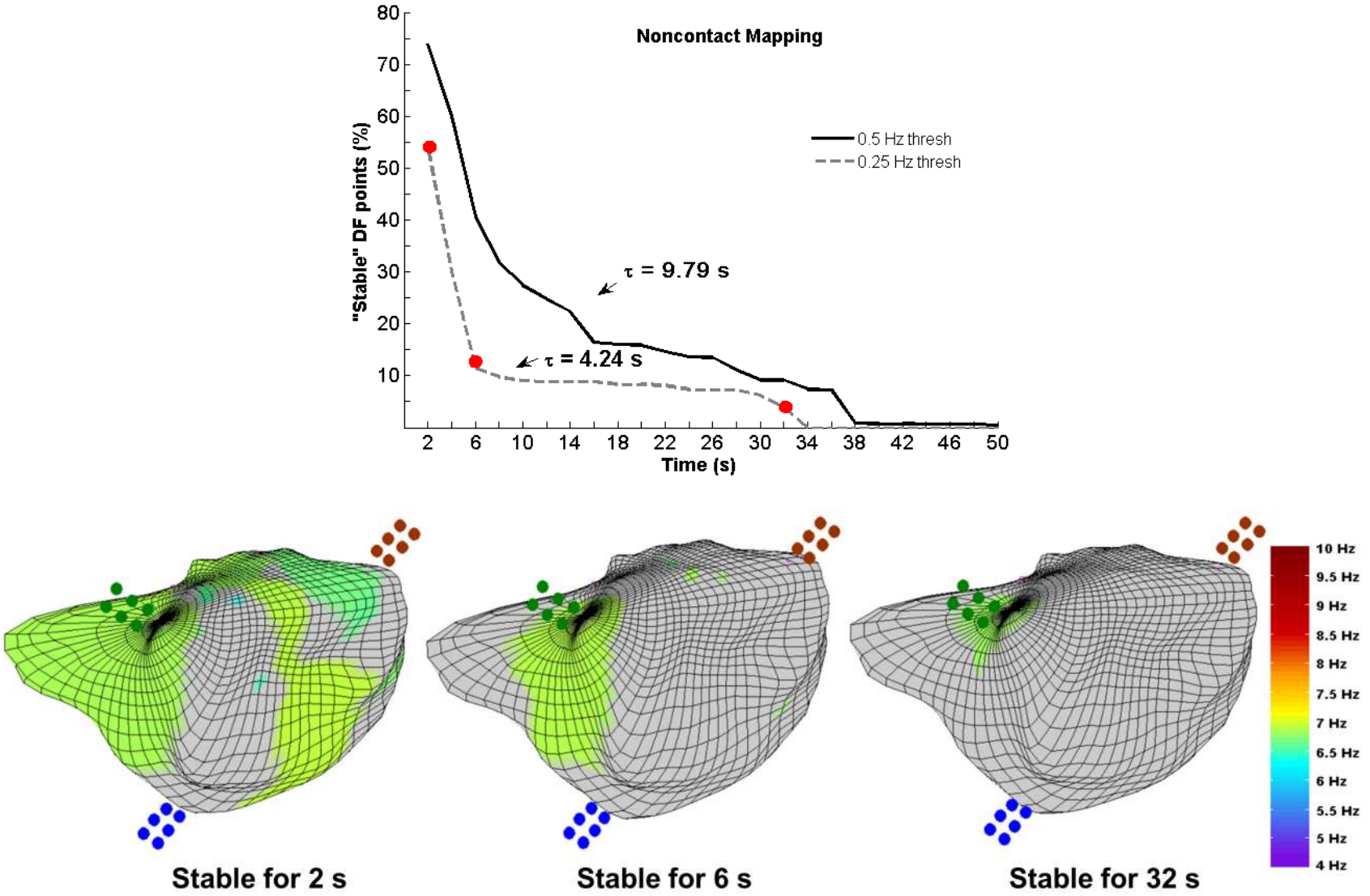
Noncontact Mapping
"Stable" DF points (%)
Time (s)
0.5 Hz thresh
0.25 Hz thresh
τ = 9.79 s
τ = 4.24 s
Stable for 2 s
Stable for 6 s
Stable for 32 s
10 Hz
9.5 Hz
9 Hz
8.5 Hz
8 Hz
7.5 Hz
7 Hz
6.5 Hz
6 Hz
5.5 Hz
5 Hz
4 Hz

Figure 4

(A)

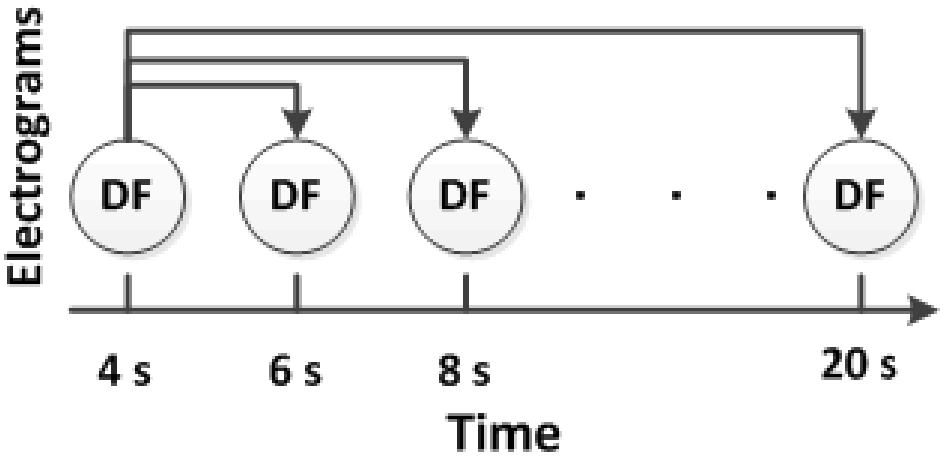

Figure 4B

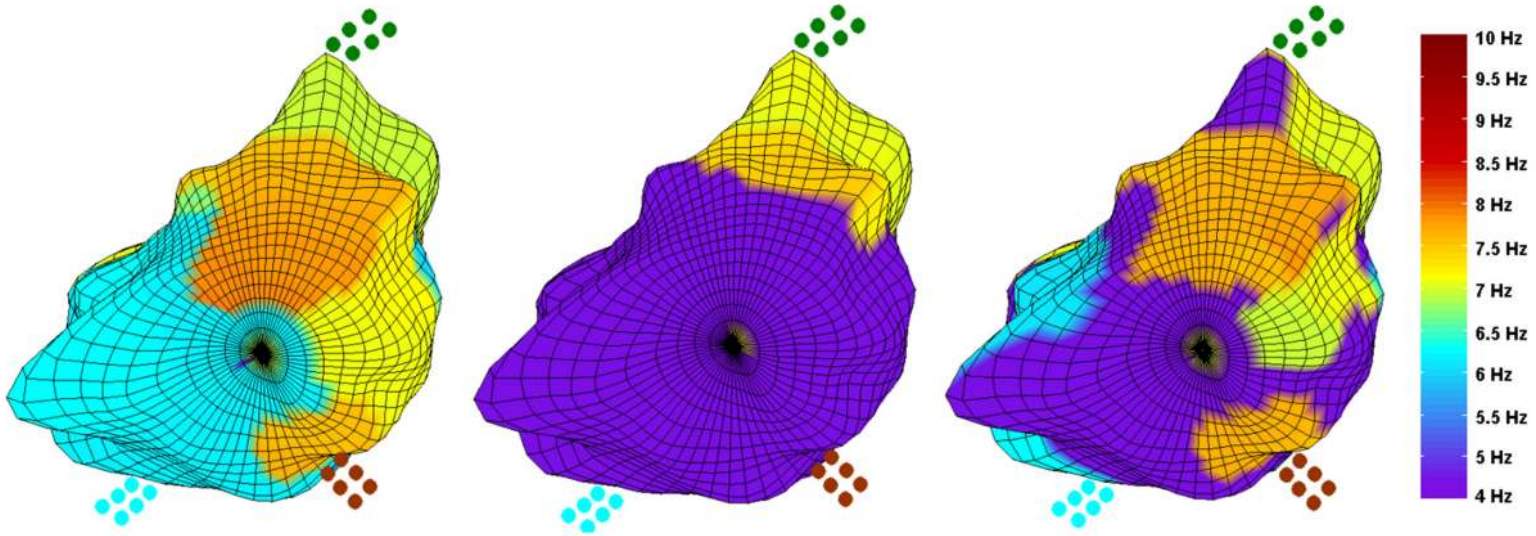

4 s 10 s 18 s

Figure 4C

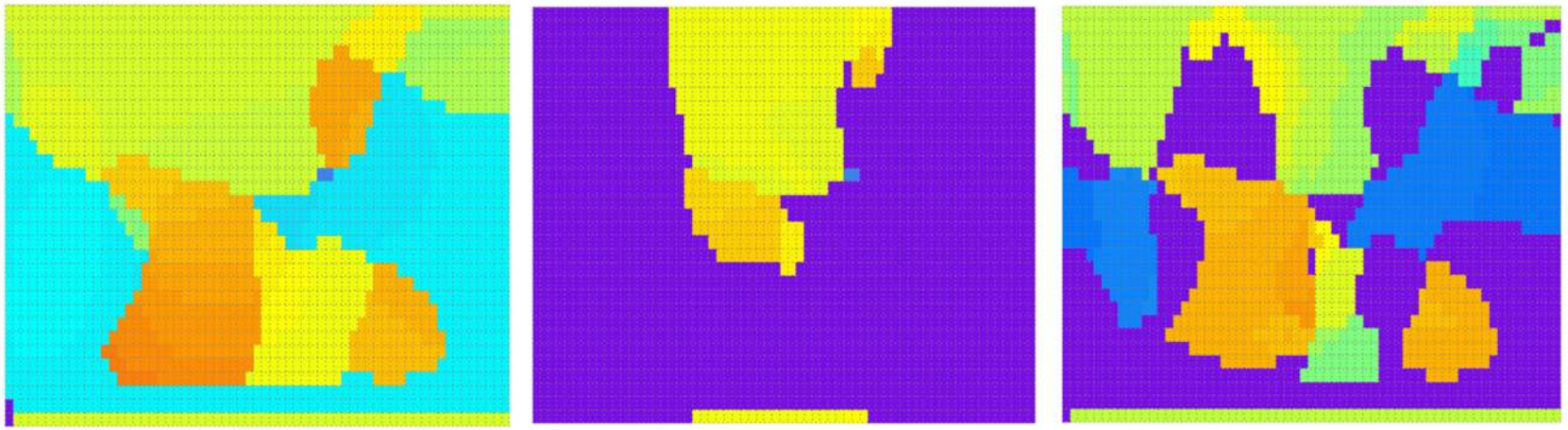

Figure 5A

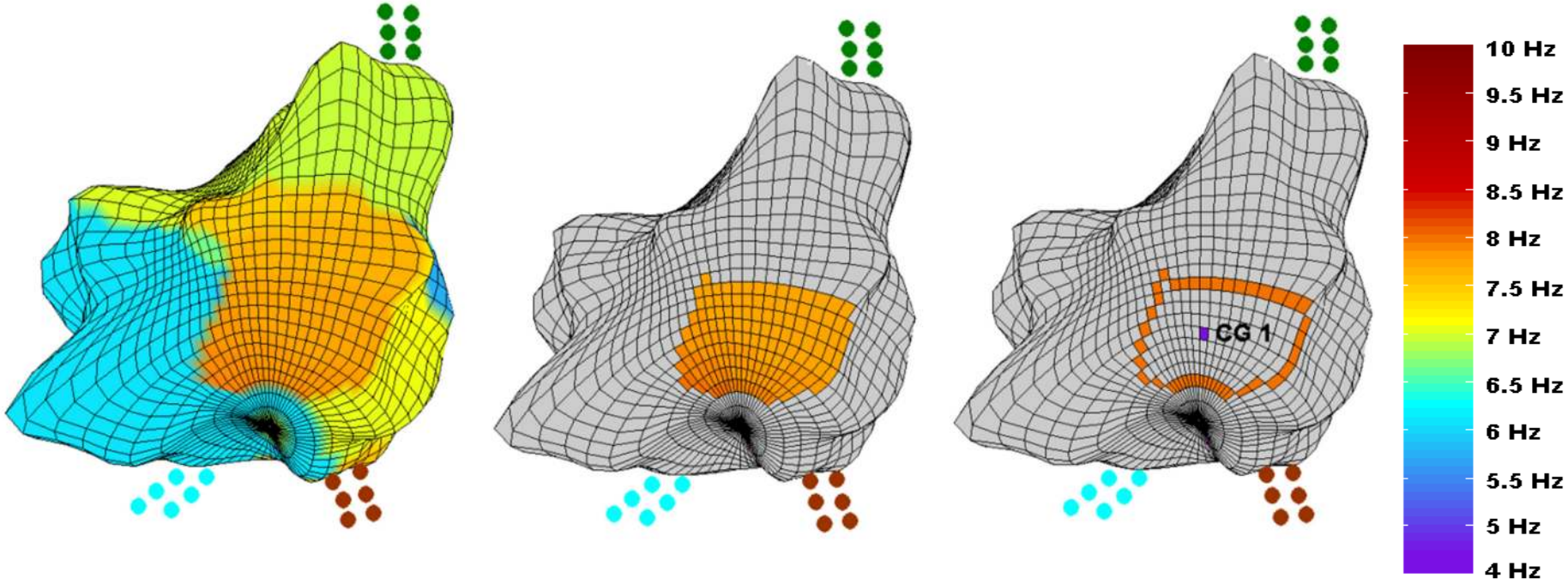

Figure 5B

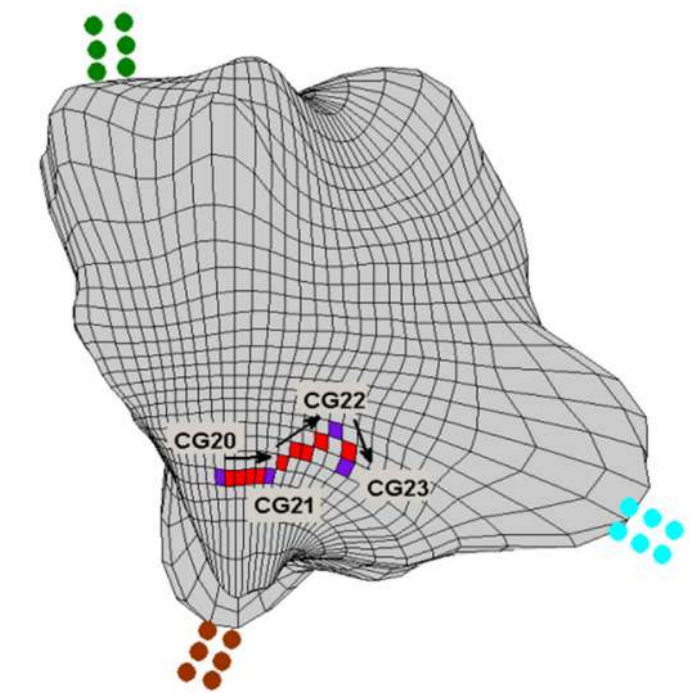

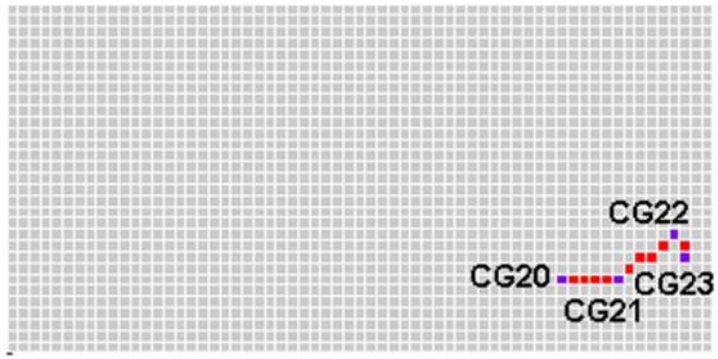

Localised

Figure 5C

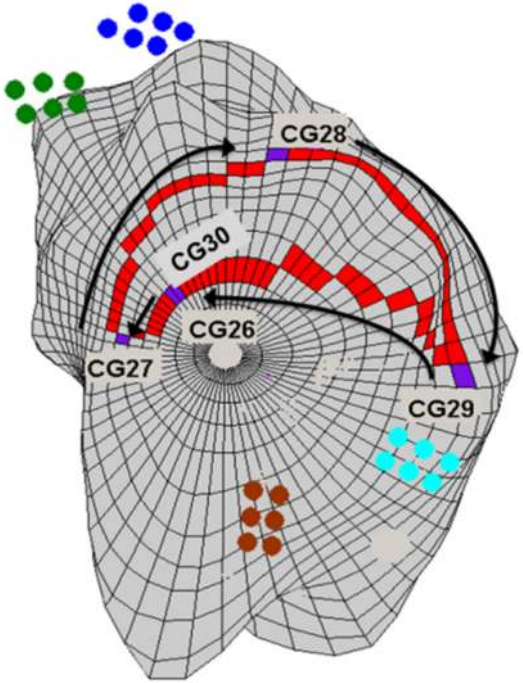

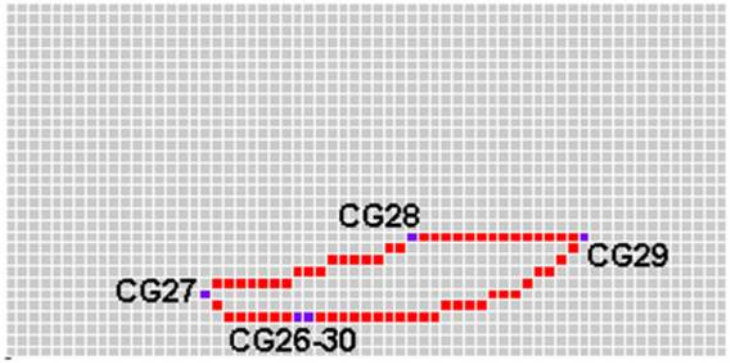

Cyclical

Figure 5D

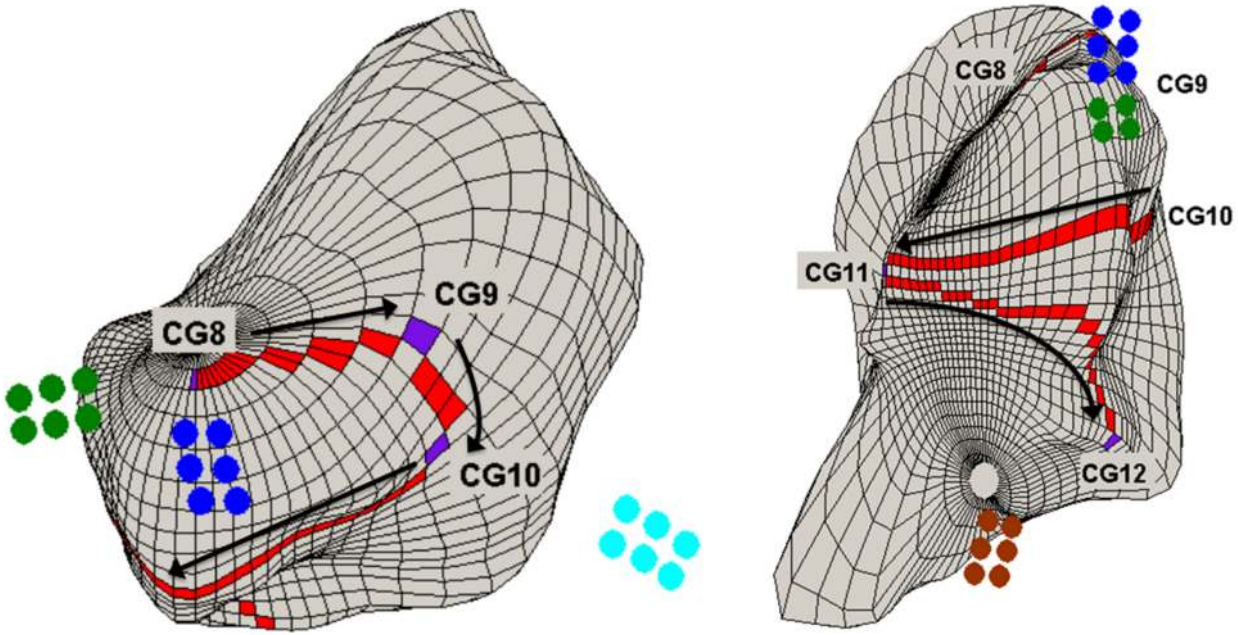

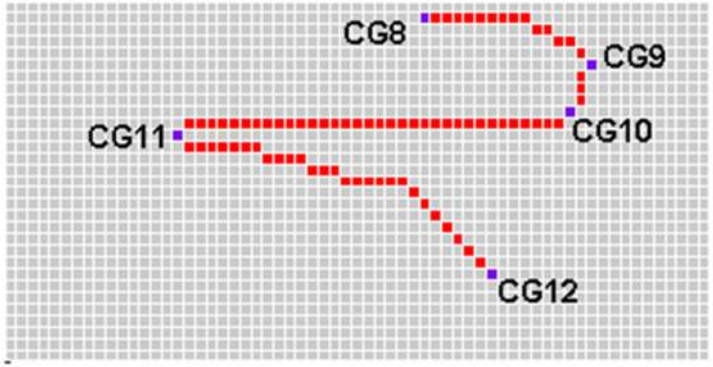

Chaotic